Contract No:

This document was prepared in conjunction with work accomplished under Contract No. DE-AC09-08SR22470 with the U.S. Department of Energy.

Disclaimer:

Corrosion Testing of Carbon Steel in Oxalic Acid that Contains Dissolved Iron

B. J. Wiersma and J. I. Mickalonis
Savannah River National Laboratory
Savannah River Nuclear Solutions
Aiken, South Carolina 29808

K. H. Subramanian
Savannah River Remediation
Aiken, South Carolina 29808

ABSTRACT

Radioactive liquid waste has been stored in underground carbon steel tanks for nearly 60 years at the Savannah River Site. The site is currently in the process of removing the waste from these tanks in order to place it into vitrified, stable state for longer term storage. The last stage in the removal sequence is a chemical cleaning step that breaks up and dissolves metal oxide solids that cannot be easily pumped out of the tank. Oxalic acid (OA) will be used to chemically clean the tanks after waste retrieval is completed. The waste tanks at SRS were constructed from carbon steel materials and thus are vulnerable to corrosion in acidic media. In addition to structural impacts, the impact of corrosion on the hydrogen generated during the process must be assessed. Electrochemical and coupon immersion tests were used to investigate the corrosion mechanism at anticipated process conditions. The testing showed that the corrosion rates were dependent upon the reduction of the iron species that had dissolved in solution. Initial corrosion rates were elevated due to the reduction of the ferric species to ferrous species. At later times, as the ferric species depleted, the corrosion rate decreased. On the other hand, the hydrogen evolution reaction became more dominant.

Keywords: carbon steel, radioactive waste tanks, oxalic acid, chemical cleaning

INTRODUCTION

Radioactive liquid waste has been stored in underground carbon steel tanks for nearly 60 years at the Savannah River Site (SRS). The site is currently in the process of removing the waste from these tanks in order to place it into a vitrified, stable state for longer term storage. The last stage in the removal sequence is a chemical cleaning step that breaks up and dissolves metal oxide solids that cannot be easily pumped out of the tank. Oxalic acid (OA) has been selected for this purpose because it is an effective chelating agent for the solids and is not as corrosive to the carbon steel tank as other acids.

The chemical cleaning process follows the basic general steps:

- Add 8 wt.% Oxalic Acid (OA) to the residual sludge heel at up to 75 °C
    - The volume ratio of OA to sludge must not exceed 20:1 (limited by the ratio of OA during laboratory testing conditions)
- Add well water to dilute the OA to desired concentration (nominally ≤4 wt.%)
- Operate mixing pumps
    - The maximum temperature during pump operation is 60 °C
- Transfer slurry to receipt tank for neutralization.

This evolution is a deliberate process, and each strike (i.e., there are typically up to 3 acid strikes) will be completed within approximately 14 days. The initial addition of 8 wt.% OA will take 2 or 3 days to complete. Water addition to dilute the solution to ≤ 4 wt.% and minimum mixing level will require an additional 1 to 5 days.

Mixing pumps will be operated for 2 to 7 days, and the transfer to the receipt tank will take an additional 2 to 3 days. The total time per strike will be approximately 14 days.

Corrosion rate data for carbon steel exposed to the chemical cleaning environment were needed to evaluate the degree of degradation that could occur in the treatment tank during this process and the propensity for hydrogen evolution due to the corrosion of carbon steel. The corrosion tests involved concurrent electrochemical and coupon immersion testing. The electrochemical studies were typically performed to gain a better understanding of the corrosion mechanism, particularly the influence of the ferric species in solution. The coupon immersion tests were performed under environmental conditions that were as representative of the actual process as possible. The coupons were examined for weight loss and any evidence of localized corrosion. The corrosion rates obtained from these tests will be utilized for estimates for the actual process.

EXPERIMENTAL

Test Materials

The coupon material used for the tests was ASTM A285, Grade C carbon steel (UNS K02200). This material has similar chemical and physical properties to the waste storage tanks that will be the focus of the initial chemical cleaning operations. The chemical composition (see Table 1) of the as-received coupons was vendor certified. The dimensions of each coupon were measured with digital calipers to the nearest 0.025 mm (or 0.001 inches). The coupons were weighed on an analytical balance to the nearest 0.0001 grams.

Two types of samples were tested. The first was a rectangular, flat coupon approximately 1" X 2" X 0.25". The flat coupon simulates the un-welded base metal of the tank and will be examined for general and pitting corrosion. The initial surface condition of the coupons was a 600 grit polished finish. The polished coupons provide a uniform, reproducible surface finish ideal for studying reactions between the steel and the environment.

Table 1. Chemical Composition (Wt %) of A285 Grade C, Carbon Steel

C	Mn	P	S	Cu	Ni	Cr	Si	Fe
0.18	0.75	0.011	0.008	0.03	0.03	0.06	-	balance

In-situ monitoring of the corrosion process during the test was performed with electrochemical probes. The electrochemical probes were prepared from the same A285 carbon steel material as the coupons. The pre-mounted probe was nominally 0.25" x 0.25" x 0.3" (i.e. 0.425 in^2 or 2.73 cm^2). The probe was prepared for testing by attaching a 22 AWG wire to one end of a coupon with silver epoxy. The probe was then mounted in a chemically resistant acrylic compound to protect the exposed end of the wire and the silver epoxy during the test and to provide an easily held sample (see Figure 1). After the probe was mounted, the exposed area of the probe was measured to determine the surface area. The surface areas for the eight probes that were prepared for the tests ranged from approximately 1.6 to 2.79 cm^2.

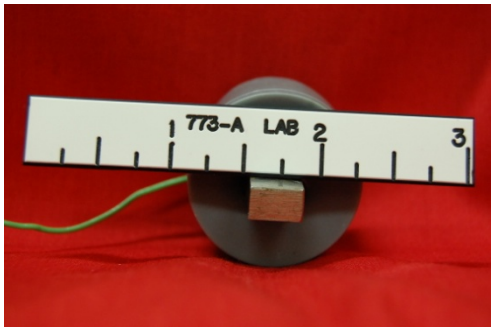

(a)

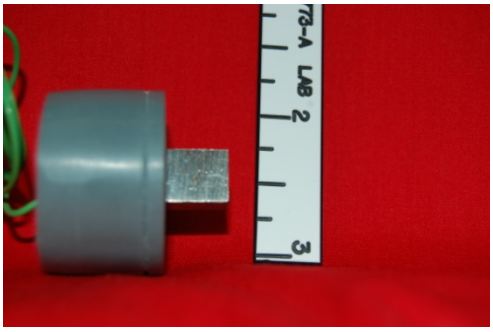

(b)

Figure 1. Electrochemical probe for tests (a) End View and (b) Side View.

Test Solutions

The sludge simulant for these tests was developed based on sludge samples obtained from the tank prior to aluminum dissolution operations. The sludge was comprised primarily of aluminum, iron, and manganese oxides. A partial listing of the primary constituents of the sludge is shown in Table 2. The listing compares the concentrations from the actual sludge sample with those from the simulant on a sludge slurry basis. The differences in the concentrations were minor for the major components such as aluminum and iron. There were some differences noted for the sodium and manganese concentrations. The difference in the sodium concentrations was due to washing procedures utilized during the preparation of the sludge simulant that removed soluble sodium species since the sample from the tank was obtained before the solids were washed. The manganese concentration in the simulant was approximately twice that of the sample from the tank. For the simulant, potential redox active species such as manganese were based on the sludge composition in another tank. The customer requested this higher concentration for process considerations.

The tests were conducted at four conditions as shown in Table 3. The ratio of OA to sludge on a volume basis for each of the four tests was approximately 20:1, while the OA concentration was varied between 2.5 to 8 wt.% OA. Temperatures for these tests ranged between 60 and 75 °C.

The pH of the OA/HM sludge simulant was monitored each day. Initially all solutions were at a pH between 1 and 1.5. However, after a day or so the pH in vessels 1 and 4 (i.e., 4 wt.% OA and 2.5 wt.% OA, respectively) began to increase. In an effort to promote sludge dissolution, additional acid at the same initial concentration was added to these vessels in order to maintain the pH below 2. However, after approximately 600 ml of acid (i.e., 1 week of testing) had been added to the vessel, the pH did not stabilize below 2 and the maximum volume of the vessel was nearly exceeded. Therefore further additions to these two vessels were not made.

During the test, the solution composition for each vessel was determined at 1, 3 and 4 weeks, which coincided with the planned interval tests. The aluminum, iron, and mercury concentrations were of particular interest as these constituents appeared to have played a role in the corrosion that was observed during previous testing.

Table 2. Primary Constituents of Sludge Obtained from Tank and the Simulant Utilized for Testing.

Constituent	Actual Sludge (wt.% solids on a slurry basis)	Sludge Simulant (wt.% solids on a slurry basis)
Al	11	10.4
Ca	0.22	0.245
Fe	1	1.03
Hg	0.39	0.409
Mg	0.21	0.22
Mn	0.47	1
Na	30	2.12
Si	0.04	0.022

Table 3. Test Matrix for Coupon Immersion Tests

Test	Wt.% OA	Temperature (°C)	Agitation	Simulant
1	4	60	Y	HM

2	8	60	Y	HM
3	8	75	N	HM
4	2.5	60	Y	HM

Experimental Procedures

Electrochemical Tests.

The tests with the electrochemical probes were performed over four weeks concurrently with the coupon tests. To perform the corrosion measurements within each test vessel, an electrochemical cell was designed. The cell consisted of four primary features: a) a working electrode, b) a counter electrode, c) a reference electrode, and d) a potentiostat. Each feature is briefly described below.

The working, or corroding, electrode is the carbon steel probe. Two working electrodes were positioned in a glass "tree-like" holder with the face oriented approximately perpendicular to the bottom of the vessel (see Figure 2). The wires from the coupons were extended through the top of the vessel via a glass tube, where they were then attached to the potentiostat.

In these tests carbon graphite rods served as the counter electrodes. A 22 AWG wire was attached to one end of the rod with silver epoxy and covered with the acrylic mounting material. The counter electrodes were positioned to allow for a uniform current density to flow from the working electrodes (see Figure 2). Two rods were oriented vertically in the vessel such that the two probes were flanked on each side by a counter electrode. The wires from the counter electrodes extended through the top of the vessel via the glass tube for connection to the potentiostat.

These tests used a saturated silver/silver chloride (sat. Ag/AgCl) electrode. This electrode has shown excellent stability and reproducibility in previous high temperature testing with similar chemical systems. The reference electrode was held by a separate glass tube holder and fully immersed in the solution near the tree-like holder, away from the large sample (see Figure 2). The wire from the reference electrode extended through the top of the vessel via the glass tube for connection to the potentiostat.

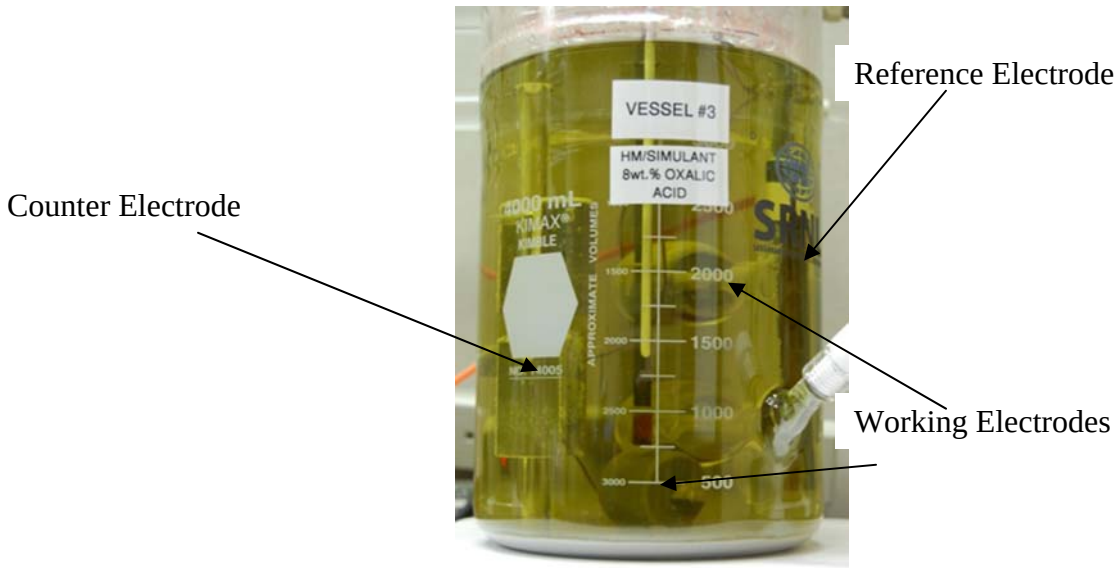

Figure 2. Cell set-up for electrochemical tests.

The potentiostat utilized for these tests was a Gamry™ PCI4/750 Potentiostat/Galvanostat/Zero Resistance Ammeter. The potentiostat was connected to a Gamry™ ECM8 Electrochemical Multiplexer, so that multiple working electrodes could be monitored simultaneously. A laptop computer was used to interface between the potentiostat and the multiplexer. The data acquisition software was Framework Version 5.6 supplied by Gamry™.

The electrochemical tests performed include: 1) Open circuit potential (OCP) measurement, 2) Linear polarization resistance (LPR) measurements, and 3) Cyclic potentiodynamic polarization (CPP). A brief description of the relevance of the data and how the data was collected is presented.

The OCP reflects a measure of the electrochemical activity at the metal surface, i.e. whether it is actively corroding or becoming passive. The test also provides information on the relative stability of the passive film, and whether hydrogen evolution is thermodynamically possible. For these tests, the OCP was monitored periodically (i.e., 3 to 4 hours) during the four week test to determine if changes in the passive film or environment may lead to a propensity for hydrogen evolution at any time during the test.

The potentiostat software was programmed to collect the OCP data in a sequential manner from each of the eight probes. That is, the OCP for probe 1 in vessel 1 was measured for a short time followed by probe 2 in vessel 1 being measured, and so forth. The cycle for the eight probes was repeated every 3 to 4 hours. It should be noted however, that there were gaps where no data was taken over weekends.

The linear polarization test was performed in conjunction with the OCP monitoring. The LPR technique provides a non-destructive, instantaneous estimate of the uniform or general corrosion rate at a given specific time. The ASTM standard practice was utilized to conduct the test [1]. The potential was scanned from -0.020 V to +0.020 V vs. OCP. A scan rate of 0.167 mV/s was selected for these tests.

Cyclic potentiodynamic polarization (CPP) was the final electrochemical test that was performed. The CPP test was initiated at a potential approximately 200 mV less than the E_{corr} at a given time. A sequentially increasing potential was applied to the probe at scan rate of 0.167 mV/s. The current response to the change in potential is measured to establish a current-potential relationship. At a potential approximately 1 V above the E_{corr}, the scan was reversed such that a sequentially decreasing potential is applied to the probe at the same scan rate. To obtain data at a later time in the test another probe was employed, or sufficient time is allowed for the sample to re-establish equilibrium. In these tests, CPP curves were performed after 2 and 4 weeks of exposure.

The CPP curve was utilized for two purposes. The first analysis involved the cathodic region of the CPP plot, which extends from Ecorr to more negative potentials. This region was used to investigate the kinetics of the cathodic electrochemical reaction. From these studies, the propensity for hydrogen may be investigated. The dominant term controlling the corrosion rate for many metals exposed to non-oxidizing acids, such as oxalic acid, is hydrogen overvoltage at cathodic areas of the metal. Hydrogen overvoltage is the difference of potential between a cathode at which hydrogen is being evolved, and a hydrogen electrode at equilibrium in the same solution. The rate at which hydrogen evolution occurs depends on the catalytic properties of the electrode surface. A relatively pure iron corrodes at a low rate compared to a surface that contains impurities such as carbon, sulfur and phosphorous, which catalyze the hydrogen reaction [2].

To determine if hydrogen is the dominant cathodic reaction the following relationship was utilized [2]:

$$\alpha = 2.3\ R\ T/(\beta\ F) \qquad (1)$$

where α is the transfer coefficient, R is the universal gas constant equal to 8.314 J/mole-K, T is the temperature in K, and F is the Faraday constant equal to 96,500 J /equivalent. For iron and steel, α is approximately 0.4 to 0.6 if the hydrogen reaction is occurring at the surface [2]. If α is significantly less than 0.4, this is typical of a cathodic reaction that is diffusion controlled (i.e., β approaching infinite values). That is, the rate of cathodic reaction is dependent upon diffusion of the oxidizer to the electrode surface.

The cathodic region of the scan will be investigated to determine which reactions are possibly dominant. Of particular interest is the potential at which hydrogen evolution appears to be the clearly dominant cathodic reaction. This potential, defined as E_h, is determined empirically from the cathodic region of the CPP plot as shown in Figure 3. Below this potential the slope of the line on the potential-log current density plot is such that α from Equation 1 is approximately 0.4 to 0.6. For potentials at or below this value, hydrogen is the dominant cathodic reaction on the steel surface.

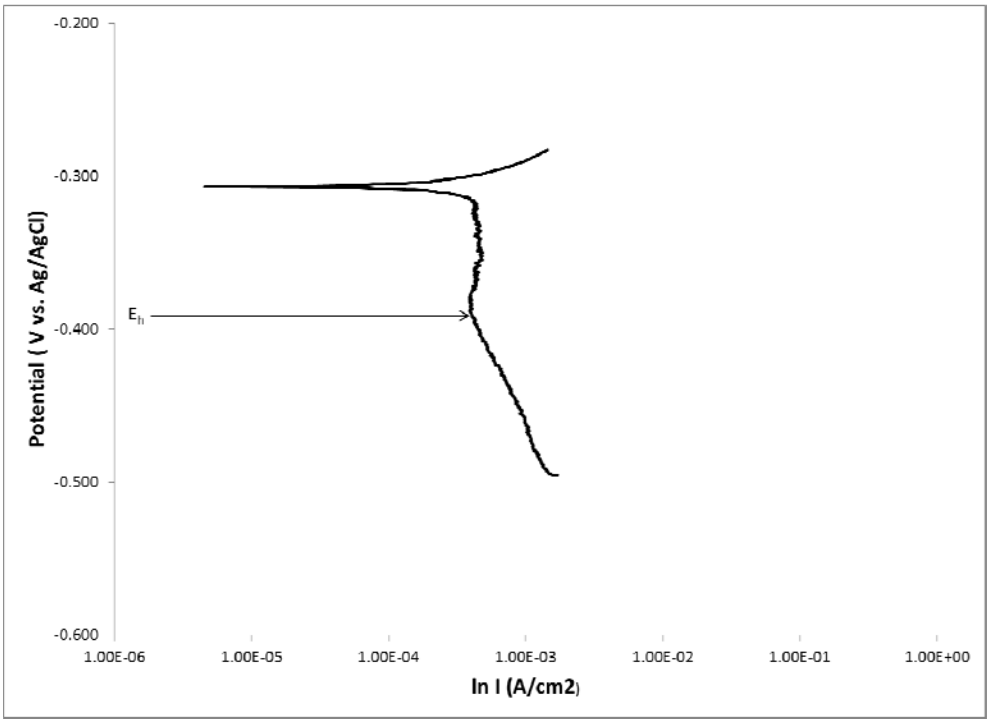

Figure 3. Cathodic region of the CPP curve showing the empirically determined E_h.

Various current responses that occur during the anodic or forward scan have been shown to be indicative of localized corrosion susceptibility. In particular, the breakdown potential, E_b, is the potential where the current increases rapidly with a small change in potential. This change has been correlated with a reduction in the passive nature of the material. The smaller the difference between values of E_{corr} and E_b, the more susceptible the material is to localized corrosion in that environment. The passive current density, I_p, is also indicative of the protective nature of the oxide film, or in this case the oxalate film. Lower passive current densities are indicative of a more stable protective film.

Data from the reverse scan as well as the forward scan are utilized to determine susceptibility to localized corrosion. If the current density of the reverse scan is greater than that for the forward scan, localized corrosion is likely. This behavior is known as positive hysteresis and indicates that pits have formed and are continuing to propagate. If the current density of the reverse scan is less than that for the forward scan, passive behavior is

expected. This behavior is known as negative hysteresis and indicates that the passive film has re-formed on the surface.

Coupon Immersion Tests

Changes in the solution corrosivity (i.e., aggressiveness of the environment) and alloy corrodibility (i.e., corrosion susceptibility, passive layer formation and/or degradation, etc.) can be determined with a planned interval testing program per ASTM G31 [3]. Four flat, rectangular coupons were initially exposed to the corrosive environment of interest. Coupon number 1 was removed after 1 week of exposure, coupon number 2 after 3 weeks of exposure, and coupon number 3 after 4 weeks of exposure. Coupon number 4 was inserted for week 4 of the test.

General corrosion was evaluated by practices described in ASTM G31. The corrosion products were removed from the sample by a two-step process. First, loose corrosion products were removed using a soft wire brush. The coupons were then immersed in Clarke's solution (i.e., an inhibited HCl acid solution) to remove the final corrosion products. After removal of the corrosion products, the coupons were weighed on an M&TE calibrated balance to determine the resultant weight loss.

The extent of pitting corrosion was characterized utilizing Standard Guide ASTM G46 for Examination and Evaluation of Pitting Corrosion [4]. The examination began with visual observations of the surface to determine the morphology of the pits. Photographs of the surface were taken immediately after the coupon was removed from the test. The coupon was then examined to determine the composition and location of the corrosion products via a scanning electron microscope (SEM) coupled with energy dispersive spectroscopy (EDS). Once the samples were cleaned, the microscopical technique described in ASTM G46 was utilized to determine pit depths. A minimum of 20 of the largest pits were measured on the front and back face of each of the rectangular coupons.

RESULTS

Electrochemical Tests

OCP Monitoring.

The following observations were made from the results of the OCP monitoring. No electrochemical data was collected from the probes during the 8 wt.% OA/60 °C/ with mixing test due to difficulties with the cell set-up and the reference electrode. Probes were functional in the remaining three vessels and provided valuable mechanistic information.

- **Exposure: 2.5 wt.% OA/60 °C/ with mixing** – The OCP ranged between -0.173 and -0.366 V vs. Ag/AgCl reference electrode for the 28 day test. The OCP remained above E_{H2}, the potential above which hydrogen evolution is not thermodynamically possible, for all 28 days.
- **Exposure: 4 wt.% OA/60 °C/ with mixing** - The OCP ranged between +0.020 and -0.271 V vs. Ag/AgCl reference electrode for the 28 day test. The OCP remained above E_{H2}, the potential above which hydrogen evolution is not thermodynamically possible, for all 28 days.
- **Exposure: 8 wt.% OA/75°C/ without mixing** - The OCP ranged between -0.130 and -0.388 V vs. Ag/AgCl reference electrode for the 28 day test (see Figure 4). The OCP remained above E_{H2}, the potential above which hydrogen evolution is not thermodynamically possible, for the first 72 hours of the test. Between 72 and 400 hours the potential decayed into a region where the hydrogen generation reaction was thermodynamically stable however, the hydrogen generation rates would be negligibly low due to the large driving force required for the hydrogen evolution reaction (i.e., reaction was kinetically limited). The potential was relatively constant at approximately -0.290 V vs. Ag/AgCl during

this time. Between 400 hours and 500 hours the potential decayed to approximately -0.390 V vs. Ag/AgCl and remained at this potential for the duration of the test. During this time the hydrogen evolution reaction was not only thermodynamically stable, but kinetically the dominant cathodic reaction (see discussion of CPP curves).

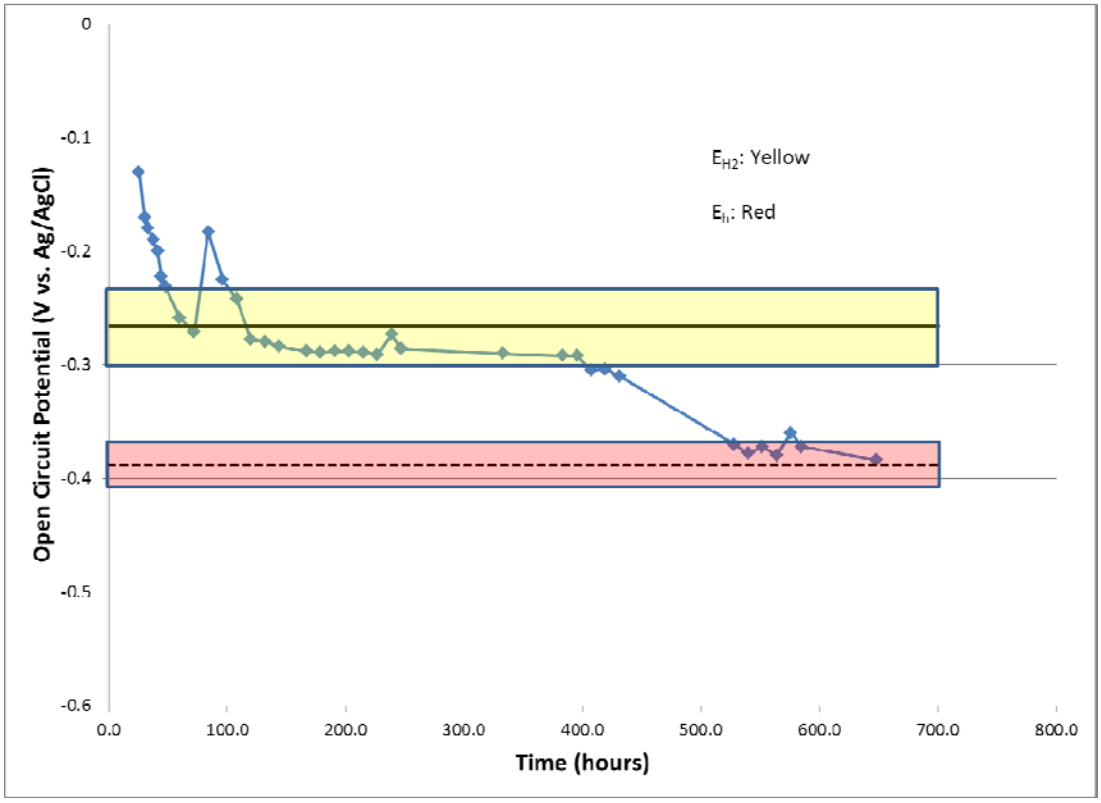

Figure 4. Open circuit potential transient for Probe #1 in HM simulant/8 wt.% OA at 75 °C with no agitation.

LPR Tests.

The following observations were made from the LPR tests.

- **Exposure: 2.5 wt.% OA/60 °C/ with mixing** – The instantaneous corrosion rate (ICR) ranged between 2.5 to 12 mpy over the 28 day test. The ICR decreased with time indicating that the solution corrosivity and/or metal corrodibility had decreased over the 28 day test. This trend was also observed for the coupon tests. The trend for the integrated ICR was the same as the time-averaged corrosion rate for the programmed interval test. The rates were typically lower by a factor of 3 to 4, however, both estimates of the corrosion rate predict a low value and given the uncertainties in the measurement of each, may actually be close.
- **Exposure: 4 wt.% OA/60 °C/ with mixing** - The ICR ranged between 2.5 to 14 mpy over the 28 day test. The ICR decreased with time indicating that the solution corrosivity and/or metal corrodibility had decreased over the 28 day test. This trend was also observed for the coupon tests. The trend for the integrated ICR was the same as the time-averaged corrosion rate for the programmed interval test. The rates were typically lower by a factor of 3 to 4, however, both estimates of the corrosion rate predict a low value and given the uncertainties in the measurement of each, may actually be close.

- **Exposure: 8 wt.% OA/75°C/ without mixing** - The ICR ranged between 15 to 137 mpy over the 28 day test (see Figure 5). The ICR initially increased and passed through a maximum between 150 and 225 hours. After that time, the ICR gradually decreased until it achieved a steady value of approximately 30 mpy after 500 hours of testing. The results indicated that the solution corrosivity and/or metal corrodibility had decreased over the 28 day test. This trend was also observed for the programmed interval test (see coupon test results). The trend for the integrated ICR was the same as the time-averaged corrosion rate for the coupons. The estimates of the time averaged corrosion rate predicted essentially the same value and are within the uncertainties of the measurement of each.

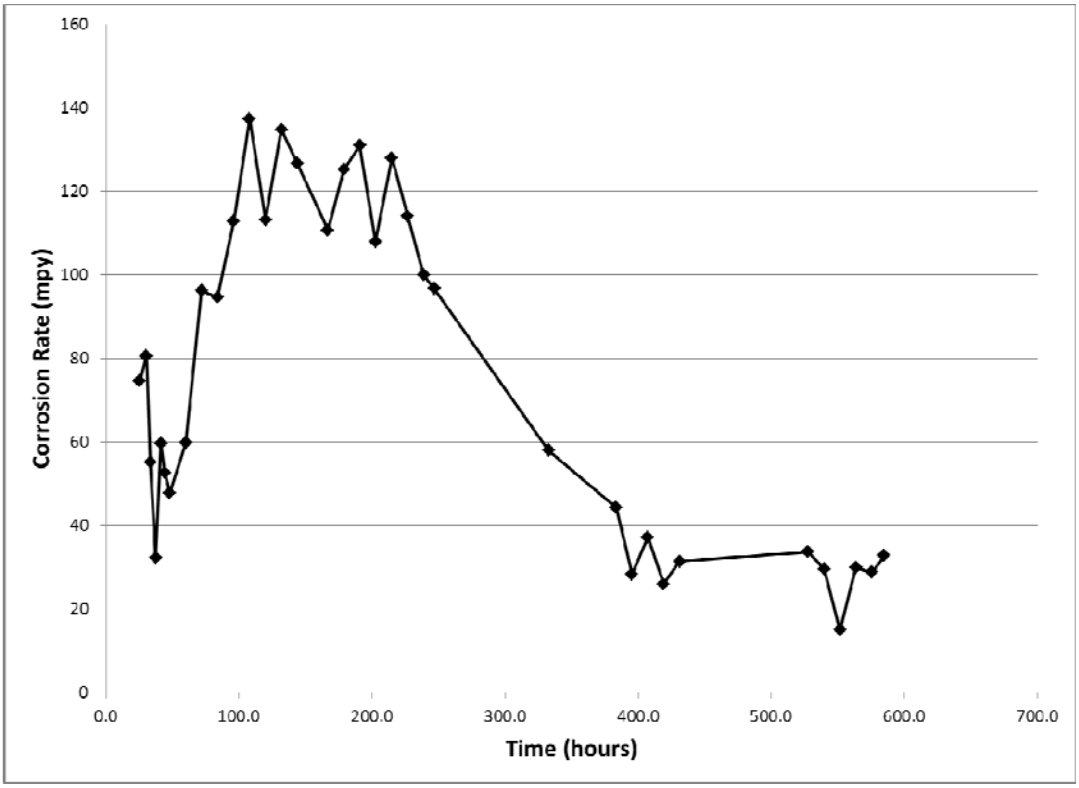

Figure 5. Instantaneous Corrosion Rate for Probe #1 HM simulant/8 wt.% OA at 75 °C with no agitation.

Cyclic Potentiodynamic Polarization.

The following observations were made from the results of the evaluation of the cathodic region of the cyclic polarization tests.

- **Exposure: 2.5 wt.% OA/60 °C/ with mixing** – The results indicated that a diffusion controlled reaction, likely reduction of the ferric oxalate complex, was limiting the corrosion rate to a low value at the time of the test. E_h was identified at approximately -0.425 V vs. Ag/AgCl at 14 days and was essentially the same value at 28 days. The value for was calculated to be 0.45, which is in the range for hydrogen evolution from a steel surface. The current density measured at 28 days was significantly less than at 14 days, indicating that solution corrosivity and/or metal corrodibility had decreased during the test. E_h was more than 0.06 V below the lowest value for the OCP during the entire test.
- **Exposure: 4 wt.% OA/60 °C/ with mixing** - The results indicated that a diffusion controlled reaction, likely reduction of the ferric oxalate complex, was limiting the corrosion rate to a low value at the time of the test. E_h was identified at approximately -0.354 V vs. Ag/AgCl. This potential was more than 0.08 V

below the lowest value for the OCP during the entire test. The value for □ was calculated to be 0.59, which is in the range for hydrogen evolution from a steel surface.

- **Exposure: 8 wt.% OA/75°C/ without mixing** - The cathodic curve at 14 days was significantly different than the curve at 28 days (see Figures 6 and 7). The 14 day curve indicated that a diffusion controlled reaction, likely reduction of the ferric oxalate complex, was limiting the corrosion rate; however, the rate was much higher than that for the other two test conditions. E_h was identified at approximately -0.384 V vs. Ag/AgCl. This potential was more than 0.08 V below the lowest value for the OCP prior to this time. The value for □ was calculated to be 0.37, which is in the range for hydrogen evolution from a steel surface. The value for □ is less than previous values mentioned and possibly reflects the fact that the reduction of ferric oxalate is still occurring at some of the cathodic sites on the surface. A difference of 0.120 V also exists between E_{H2} and E_h at this time. This difference can occur if there is another cathodic reaction that is dominant within the same region as E_{H2}. In this case, the dominant cathodic reaction was ferric oxalate reduction. The cathodic curve for the 28 day test clearly indicated that the hydrogen evolution was occurring at the OCP of -0.388 V vs. Ag/AgCl. The value for □ was calculated to be 0.60, which is in the range for hydrogen evolution from a steel surface. The rate at which the reaction occurred was much lower than the rate at 14 days. The value for E_h is approximately the same as that observed at 14 days and is well below the value for E_{H2}.

The dominant cathodic reaction at 14 and 28 days may be evaluated from these results. If the open circuit potential is more positive than the equilibrium potential for hydrogen evolution (E_{H2}), the H^+ being reduced is zero and Fe^{+3} reduction is the primary cathodic reaction. However, even when the open circuit potential is less than E_{H2}, Fe^{+3} reduction can still be the dominant cathodic reaction. The two figures below illustrate how the cathodic portion of the CPP curve may be de-convoluted to estimate how much cathodic current is due to the Fe^{+3} reduction and how much is due to H^+ reduction. Figure 6 shows the cathodic portion for the CPP after 14 days of exposure to the HM simulant/8 wt.% OA at 75 °C with no agitation. The experimental data is the red curve, the brown dashed line represents the idealized hydrogen evolution polarization kinetics, and the black dashed line represents the diffusion limited kinetics of the Fe^{+3} reduction. The sum of the currents for H^+ reduction and Fe^{+3} reduction should be approximately equal to the currents shown in the experimental curve. At E_{corr}, which is near the open circuit potential, the current due to H^+ reduction is approximately 200 times less than that for Fe^{+3} reduction. Figure 7 shows the cathodic portion of the CPP after 4 weeks of exposure to the same solution. The idealized hydrogen evolution polarization kinetics is also shown. Nearly all of the experimentally measured reduction current is expected to be due to hydrogen evolution after 28 days of exposure.

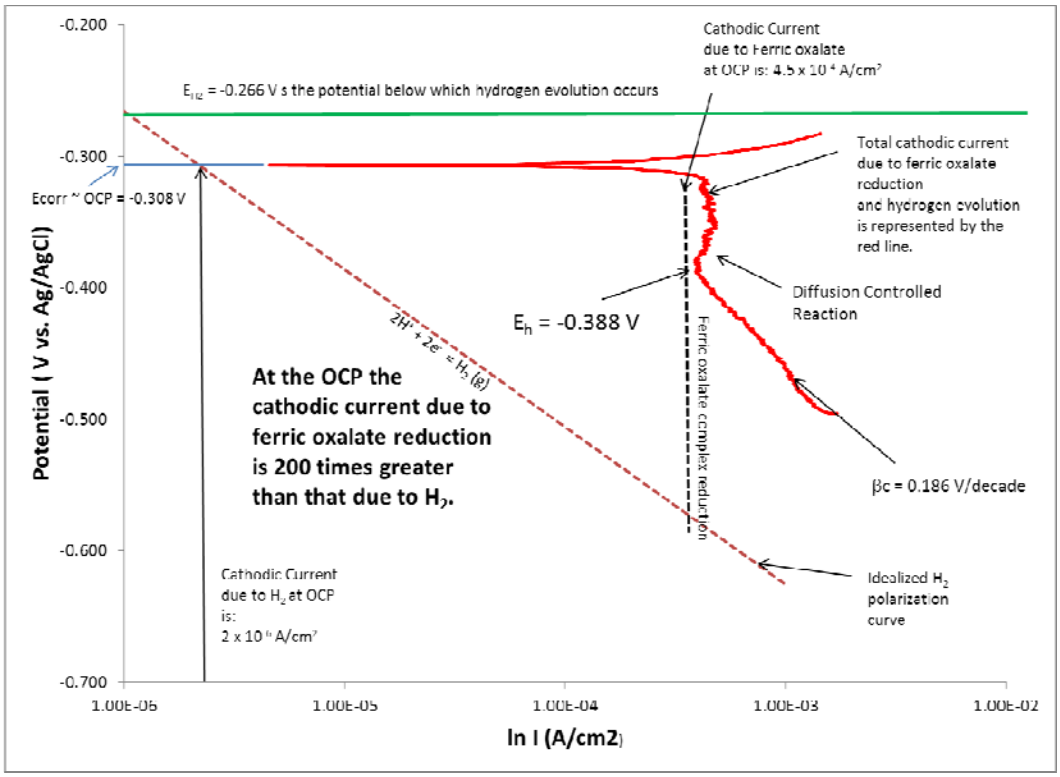

Figure 6. Fe^{+3} and H^{+} reduction kinetics at 2 weeks for HM simulant/8 wt.% OA at 75 C with no agitation.

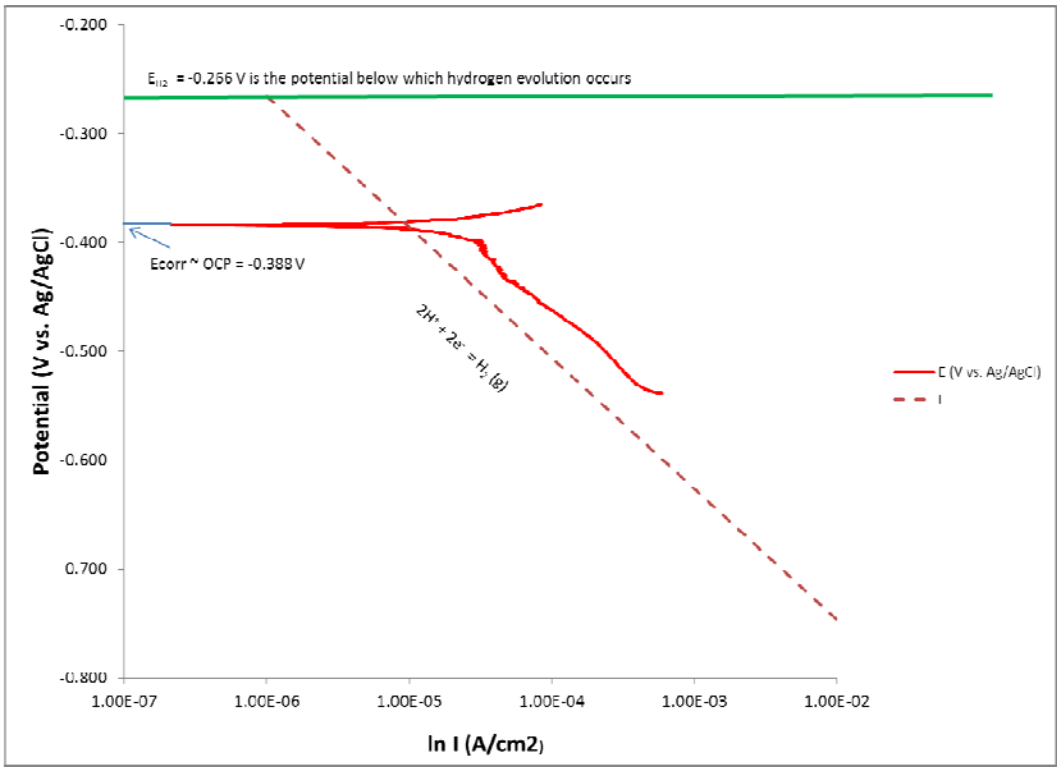

Figure 7. Fe^{+3} and H^{+} reduction kinetics at 4 weeks for HM simulant/8 wt.% OA at 75 C with no agitation.

The anodic region of the CPP scan was evaluated to investigate the metal dissolution and passivation reactions that occurred. The following observations were made from the results of the evaluation of the anodic polarization curve.

- **Exposure: 2.5 wt.% OA/60 °C/ with mixing** – The results for the 14 day test indicated passivation of the surface with ferrous oxalate occurred rapidly near the OCP. Passive behavior was exhibited over a relatively large range of potentials (approximately 0.6 V). Breakdown of the ferrous oxalate film was observed at +0.400 V vs. Ag/AgCl. Lower current densities were observed for the 28 day test than were observed for the 14 day test. This result indicated that the solution corrosivity during this test decreased with time.
- **Exposure: 4 wt.% OA/60 °C/ with mixing** - The results indicated passivation of the surface with ferrous oxalate occurred rapidly near the OCP. Passive behavior was exhibited over a relatively large range of potentials (approximately 0.6 V). Breakdown of the ferrous oxalate film was observed at +0.400 V vs. Ag/AgCl. Higher current densities were observed for this test than the 2.5 wt.% OA test. This result indicated that the 4 wt.% OA solution was slightly more corrosive than the 2.5 wt.% OA solution.
- **Exposure: 8 wt.% OA/75°C/ without mixing** - The anodic curve at 14 days was significantly different that the curve at 28 days (See Figures 8 and 9). For the 14 day test, a current peak was observed at potentials just above OCP. The maximum current density was 4.2×10^{-3} A/cm^2. During the current increase, metal dissolution and ferrous oxalate formation occurred. This current density changed gradually with potential and increased to approximately 1.8×10^{-3} A/cm^2 at just below + 0.400 V. The gradual increase suggests that the ferrous oxalate film that formed rapidly in the anodic nose was not as stable. Breakdown of the passive ferrous oxalate film occurred at approximately + 0.400 V vs. Ag/AgCl. At 28 days, no active peak was observed at potentials just above the OCP. The current density was much lower than that at 14 days. The lower current density suggests that during the two week interval between the CPP scans, the concentration of this species has been depleted and therefore can only support lower corrosion rates.

The reverse scan of the CPP was evaluated to investigate how the passive ferrous oxalate film reforms. The following observations were made from the results of the evaluation of the reverse scan.

- **Exposure: 2.5 wt.% OA/60 °C/ with mixing** – The results indicated that the ferrous oxalate film re-formed and significant pit propagation did not occur. However, the lack of clear negative hysteresis suggests that the film was not very stable.
- **Exposure: 4 wt.% OA/60 °C/ with mixing** - The results indicated that the ferrous oxalate film re-formed and significant pit propagation did not occur. However, the lack of clear negative hysteresis suggests that the film was not very stable.
- **Exposure: 8 wt.% OA/75°C/ without mixing** - Negative hysteresis was observed for these tests (see Figures 8 and 9); that is the passive film had a tendency to re-form and pit propagation would not be predicted. The presence of ferric oxalate in solution likely accelerates the anodic reaction so that ferrous oxalate is precipitated and the current density on the reverse scan is suppressed. This result supports the previous observation that pitting corrosion was not associated with the breakdown of the ferrous oxalate film at noble potentials.

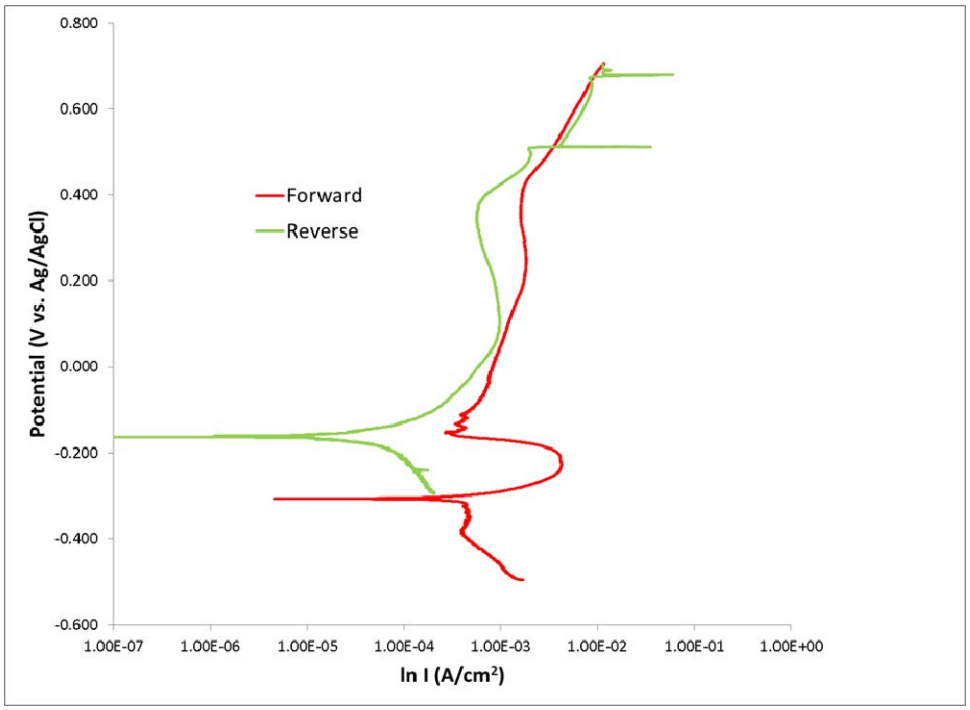

Figure 8. CPP scan for HM simulant/8 wt.% OA at 75 °C with no agitation at 2 weeks.

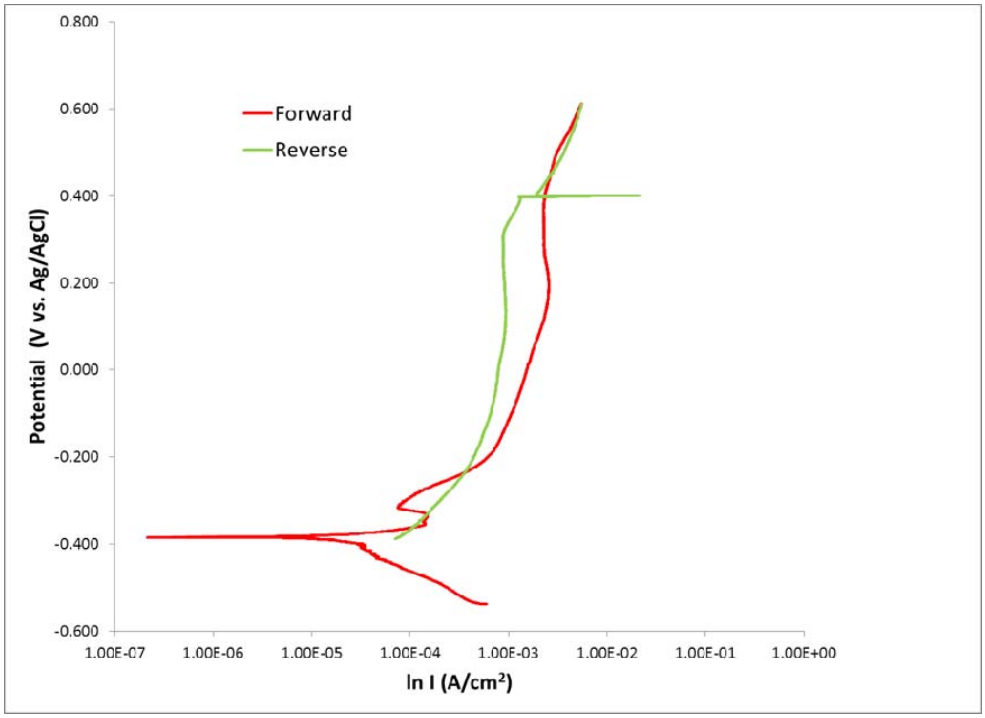

Figure 9. CPP scan for HM simulant/8 wt.% OA at 75 °C with no agitation at 4 weeks.

Coupon Test Results

The corrosion data from the coupon tests are shown in Table 1. The general corrosion rates were the time-averaged or historical rate by the gravimetric (i.e., weight loss) method. For comparison, the ICR from the LPR tests are also shown in the table.

The following observations on general corrosion were made from the coupon test results.

- **Exposure: 2.5 wt.% OA/60 °C/ with mixing** - The maximum general corrosion rate was 29 mpy for a coupon that was exposed for 1 week. The general corrosion rates decreased to 22 mpy for coupons that were exposed up to four weeks. This decrease for the time-averaged corrosion rate occurred due to a decrease in the solution corrosivity.
- **Exposure: 4 wt.% OA/60 °C/ with mixing -** The maximum general corrosion rate was 45 mpy for the coupon that was exposed for 1 week. The general corrosion rates on coupons that were exposed for up to 4 weeks decreased to 27 mpy. This decrease for the time-averaged corrosion rate was due to a decrease in both the solution corrosivity and the metal corrodibility**.**
- **Exposure: 8 wt.% OA/60 °C/ with mixing** - The maximum general corrosion rate was 93 mpy for a coupon that had been exposed for 4 weeks. The general corrosion rates at this condition increased as the exposure time increased. This increase in the time-averaged corrosion rate occurred due to an increase in the solution corrosivity and/or the metal corrodibility. This test had the high initial acid concentration and the solution was agitated. Agitation likely interfered with the build-up of the passive ferrous oxalate film, which resulted in more aggressive attack at the later stages of the test.
- **Exposure: 8 wt.% OA/75°C/ without mixing** - The maximum general corrosion rate was 141 mpy for a coupon that was exposed for 1 week. The general corrosion rates decreased as the exposure time increased so that the corrosion rate for the coupon that was exposed for four weeks was 86 mpy. This decrease for the time-averaged corrosion rate was due to a decrease in both the solution corrosivity and the metal corrodibility**.**

Table 4. Summary of the General Corrosion and Pitting Data at Each Test Condition

		LPR (instantaneous; mpy)	LPR (integrated; mpy)	Gravimetric General Corrosion Rate (mpy)	Max Pit Depth (mils)	Pitting Factor	Maximum Penetration (mils)
2.5 wt% OA / 60°C / Mixing	1 day	10	10	-----	-----	-----	-----
	7 days	5 - 12	9.1	29 (25)	0.85 (1.16)	2.5 (3.4)	1.4 (1.6)
	21 days	3 - 9	6.3	25	4.1	3.9	5.5
	28 days	2.5 - 2.7	5.3	22	6.8	5	8.5
4 wt% OA / 60°C / Mixing	1 day	11.5	11.5	-----	-----	-----	-----
	7 days	5 - 14	11	36 (45)	4.4 (1.3)	7.4 (2.5)	5.1 (2.2)
	21 days	3 - 13	9.2	32	1.3	1.7	3.1
	28 days	2.5 - 3.5	7.5	27	2.1	2	4.2
8 wt% OA / 60°C / Mixing	1 day	-----	-----	20	1.5	28	1.6
	7 days	-----	-----	51	5.1	6.2	6.1
	21 days	-----	-----	70	16.5	5.1	20.5
	28 days	-----	-----	93	39	6.5	46.1
8 wt% OA / 75°C / No Mixing	1 day	75	75	140	2.4	7.3	2.8
	7 days	32 - 137	87	141	16.1	7	18.8
	21 days	26-131	83	96	34.5	7.25	40
	28 days	15-34	69	86	3.1	1.47	9.7

Values in parentheses are from duplicate coupons

The following observations on general corrosion were made from the coupon test results.

- **Exposure: 2.5 wt.% OA/60 °C/ with mixing** - The maximum general corrosion rate was 29 mpy for a coupon that was exposed for 1 week. The general corrosion rates decreased to 22 mpy for coupons that were exposed up to four weeks. This decrease for the time-averaged corrosion rate occurred due to a decrease in the solution corrosivity.
- **Exposure: 4 wt.% OA/60 °C/ with mixing -** The maximum general corrosion rate was 45 mpy for the coupon that was exposed for 1 week. The general corrosion rates on coupons that were exposed for up to 4 weeks decreased to 27 mpy. This decrease for the time-averaged corrosion rate was due to a decrease in both the solution corrosivity and the metal corrodibility**.**
- **Exposure: 8 wt.% OA/60 °C/ with mixing** - The maximum general corrosion rate was 93 mpy for a coupon that had been exposed for 4 weeks. The general corrosion rates at this condition increased as the exposure time increased. This increase in the time-averaged corrosion rate occurred due to an increase in the solution corrosivity and/or the metal corrodibility. This test had the high initial acid concentration and the solution was agitated. Agitation likely interfered with the build-up of the passive ferrous oxalate film, which resulted in more aggressive attack at the later stages of the test.
- **Exposure: 8 wt.% OA/75°C/ without mixing** - The maximum general corrosion rate was 141 mpy for a coupon that was exposed for 1 week. The general corrosion rates decreased as the exposure time increased so that the corrosion rate for the coupon that was exposed for four weeks was 86 mpy. This decrease for the time-averaged corrosion rate was due to a decrease in both the solution corrosivity and the metal corrodibility**.**

The following observations on pitting corrosion were made from the coupon test results.

- **Exposure: 2.5 wt.% OA/60 °C/ with mixing** - Pits on the samples were typically small (i.e., less than 7 mils deep) and sparsely populated (i.e., less than $2.5x10^3/m^2$). The low density and shallow depths of these pits did not appreciably increase the surface area of the coupons. Thus, if the tank wall is exposed to similar conditions a significant increase in the surface area would not be anticipated.
- **Exposure: 4 wt.% OA/60 °C/ with mixing** - Pits on the coupons were typically small (i.e., less than 5 mils deep) and sparsely populated (i.e., less than $2.5x10^3/m^2$). The low density and shallow depths of these pits did not appreciably increase the surface area of the coupons. Thus, if the tank wall is exposed to similar conditions a significant increase in the surface area would not be anticipated.
- **Exposure: 8 wt.% OA/60 °C/ with mixing** - Pits on the samples were hemispherical and were generally broad and shallow. The maximum pit depth observed after the four week test was 40 mils. Pit density on the coupon was on the order $5x10^4/m^2$. Pits began to coalesce after three weeks of exposure. The pits were broad and shallow as indicated by the pitting factor. Due to the shallow nature of the pits the surface area of the coupons did not appreciably increase. Thus, if the tank wall is exposed to similar conditions a significant increase in the surface area would not be anticipated.
- **Exposure: 8 wt.% OA/75°C/ without mixing** - Pits on the samples were hemispherical and were generally broad and shallow (see Figure 10). Pit depths after 3 weeks of exposure were on the order of 50 mils deep. Pit density on the coupon was on the order $5x10^4/m^2$. Pits began to coalesce after three weeks of exposure. The pits were broad and shallow as indicated by the pitting factor. Due to the shallow nature of the pits the surface area of the coupons did not appreciably increase. Thus, if the tank wall is exposed to similar conditions a significant increase in the surface area would not be anticipated.
- Pitting corrosion was not associated with the breakdown of the ferrous oxalate film. Rather, pitting appears to be a result of defects that were incorporated in the ferrous oxalate film as it precipitated on the surface. These defects created a local instability in the film and were preferentially attacked. These defects may be created by solids or anion species from the sludge slurry that attach to microstructural features of the steel and/or become incorporated into the ferrous oxalate film as it forms.

- During the initial stages pitting appeared to occur near manganese sulfide particles in the steel that were adjacent to mercury particles that had deposited on to the ferric oxalate film (see Figure 11).

(a) (b)

Figure 10. Coupons Exposed to 8 wt.% Oxalic Acid at 75°C with No Agitation for 3 weeks (a) Corrosion Products, (b) Cleaned Coupon.

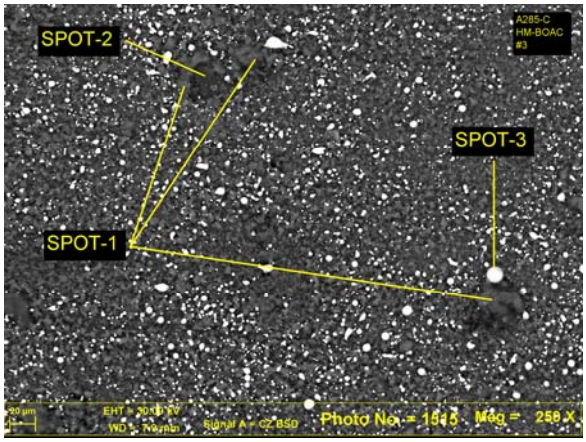

Figure 11. SEM micrograph of steel surface that had been exposed to HM/8 wt.% OA at 60 ºC for 1 day. Spot 1 and 2 are the interior of the pit. Spot 3 is deposited elemental mercury.

DISCUSSION

There are two competing cathodic reactions during corrosion of a tank wall during oxalic acid cleaning: hydrogen reduction and the reduction ferric to ferrous oxalate complex [5]. Hydrogen reduction is favored when oxygen and ferric ions are not available for reaction. However, with sludge and the iron oxides on the tank walls from mill-scale and corrosion products, ferric to ferrous oxalate reduction becomes the preferred cathodic reaction.

Open circuit potentials (OCP) and cyclic potentiodynamic polarization (CPP) tests were used to determine if hydrogen gas generation was thermodynamically or kinetically likely during the corrosion testing. These scans indicated that the periods where corrosion rates are high are due to the reduction of the ferric oxalate. None of the scenarios studied showed a potential for hydrogen generation during the first 48 hours. At 2.5 and 4 wt.%, the OCP never entered a region where hydrogen generation was thermodynamically or kinetically stable. At 8 wt. %, hydrogen generation was thermodynamically favored after 48 hours, but was kinetically limited (i.e., hydrogen may be minimally formed, but would be kinetically limited due to the other dominant cathodic reactions occurring, such as complexing of the ferric ion). After approximately 20 days hydrogen generation was favored both kinetically and thermodynamically.

The bounding corrosion induced hydrogen generation rate is based on an observed instantaneous corrosion rate of 33.6 mpy. This is the maximum observed instantaneous rate at which hydrogen generation is favored. This

rate was doubled to 67.2 mpy to account for measurement uncertainty. The cathodic reaction is conservatively assumed to only result in hydrogen evolution, resulting in a corrosion induced hydrogen generation rate of 4.3 E-05 ft^3/ft^2-min. Although higher corrosion rates were observed during the testing, hydrogen gas generation was shown to be either thermodynamically or kinetically limited at those conditions via the open circuit potential measurement. The corrosion rate of 33.6 mpy (as doubled to account for uncertainty) is the appropriate rate to use for the corrosion induced hydrogen generation rate determination because it was shown to be the highest rate where hydrogen generation was the thermodynamically and kinetically dominant cathodic reaction.

In this study, the highest corrosion rate is 141 mpy at 8 wt.% OA and 75 °C, with agitation. It should be noted that this rate was observed in the first week of the test on a polished coupon, and the rate decreased over time. Most of the process will be conducted at 4 wt.% OA or lower, and will be limited to a maximum temperature of 60 °C for pump operation. Therefore, during much of the chemical cleaning process, corrosion rates will be less than 45 mpy.

Pits on the corrosion coupons exposed to 2.5 wt.% and 4 wt.% OA were small (less than 10 mils). These pits were sparsely populated as well. Since most of the process will 4 wt.% OA or lower, pitting of the tanks is not expected to be significant during the six to eight week process. At 8 wt.% OA, the pit depth increased (up to approximately 50 mils) and the pit density was on the order of 20 times the density at the lower OA concentrations. The pits at 8 wt.% were broad, shallow and hemispherical. However, the time that the tank steel will be exposed to the higher concentration OA will occur during addition to the tank (i.e., on the order of two to three days).

CONCLUSIONS

Corrosion rate data for carbon steel exposed to chemical cleaning environment were obtained to evaluate the degree of corrosion that occurs. Electrochemical and coupon tests were performed to estimate the corrosion rate during the chemical cleaning process, the propensity for hydrogen evolution, as well as determine any susceptibility to localized corrosion.

The following recommendations for the chemical cleaning process were made based on the results of these:

- Minimize exposure time at 8 wt.% OA, 75 °C. Of the conditions that will be observed in the treatment tank, these will produce the highest corrosion rates. Although corrosion induced hydrogen generation is assumed to proceed in the waste tank at the bounding rate for the duration of the chemical cleaning process, reducing the concentration will minimize the risk of hydrogen generation and the corrosion rates of the waste tank surfaces. It is recognized that the tank structure may be degraded during the chemical cleaning process, but it is good practice to minimize damage where possible.
- Provide adequate ventilation for a corrosion induced hydrogen generation rate of 4.3 E-05 ft^3/ft^2-min in addition to the radiolytic hydrogen generation rate for the waste tank (primary and annulus).

ACKNOWLEDGEMENTS

The authors would like to acknowledge the following people for their dedicated assistance and experimental contributions to this work: K. R. Hicks, K. J. Kalbaugh, J. Durden, A. G. Hansen, and G. Dobos.

REFERENCES

1. "Standard Test Method for Conducting Potentiodynamic Polarization Resistance Measurements," ASTM G59-97, Reapproved in 2003.
2. H. H. Uhlig, Corrosion and Corrosion Control, 2nd Edition, John Wiley and Sons, NY, NY, 1971.
3. "Standard Practice for Laboratory Immersion Corrosion Testing of Metals", ASTM G31-72, 2004.
4. "Standard Guide for Examination and Evaluation of Pitting Corrosion", ASTM G46-94, 2005.
5. V. Lopez and M. J. Pena, "Electrochemical Kinetic Study of the Fe(III)-Fe(II) System in Oxalate Medium", Electrochimica Acta, Vol. 26, No. 7, pp. 857-863, 1981.